



# Null models in network neuroscience

František Váša<sup>1</sup> and Bratislav Mišić<sup>2</sup>✉

**Abstract** | Recent advances in imaging and tracing technology provide increasingly detailed reconstructions of brain connectomes. Concomitant analytic advances enable rigorous identification and quantification of functionally important features of brain network architecture. Null models are a flexible tool to statistically benchmark the presence or magnitude of features of interest, by selectively preserving specific architectural properties of brain networks while systematically randomizing others. Here we describe the logic, implementation and interpretation of null models of connectomes. We introduce randomization and generative approaches to constructing null networks, and outline a taxonomy of network methods for statistical inference. We highlight the spectrum of null models — from liberal models that control few network properties, to conservative models that recapitulate multiple properties of empirical networks — that allow us to operationalize and test detailed hypotheses about the structure and function of brain networks. We review emerging scenarios for the application of null models in network neuroscience, including for spatially embedded networks, annotated networks and correlation-derived networks. Finally, we consider the limits of null models, as well as outstanding questions for the field.

## Connectomics

The study of wiring patterns in neural systems.

## Graph

A mathematical description of a network, capturing pairwise relationships (edges) among elements (nodes).

## Degree distribution

The probability distribution of degrees (the number of connections of a node with other nodes) of all nodes in a network.

## Hub

A node with many connections.

The connectomics revolution has shifted focus to how the brain functions as a networked and integrated system<sup>1,2</sup>. Understanding the wiring principles of the brain is now the primary goal of multiple institutes<sup>3</sup>, journals<sup>4</sup> and funding initiatives<sup>5,6</sup>. Central to this pursuit is the graph model of brain structure and function, in which neural elements (such as neurons, neuronal populations or grey matter areas) are represented as nodes, and connections or interactions among them are represented as edges. Encoding neural systems as graphs enables us to quantify and articulate architectural features that are important for brain function<sup>7</sup>.

Advances in imaging technology<sup>8</sup>, analytics<sup>7,9</sup> and data sharing<sup>10</sup> provide the opportunity to describe the organization of the nervous system with unprecedented detail and depth. Over the past 15 years, convergent findings from multiple species, reconstruction techniques and spatial scales point to a core set of reproducible network features<sup>11</sup>. These include a specificity of connection profiles<sup>12,13</sup>, a heavy-tailed degree distribution, with a small set of disproportionately well-connected hub nodes<sup>14,15</sup>, and densely interconnected network modules<sup>16,17</sup>. Collectively, these network features are thought to promote a balance between segregation and integration of function<sup>18</sup>.

How do we demonstrate that a brain network feature is more prominent than would be expected by chance? Is this network feature fundamental, or does it arise as a by-product of other features? Can the magnitude of this feature be attributed to a particular

generative mechanism? Modern scientific discovery for complex systems increasingly relies on sophisticated methods of statistical inference<sup>19</sup>. Theories about important and unimportant features are operationalized as null models — alternative realizations of brain networks that possess some features but not others. Systematic comparisons between real and null networks enable researchers to disentangle dependencies between features of interest, revealing to what extent the presence or magnitude of a feature of interest arises as a consequence of other features. New discoveries are then incorporated into theories, prompting modification of existing null models. The process of refining theories by constructing progressively more stringent null models allows us to organically develop a nuanced theoretical understanding of features that are statistically unexpected and, potentially, functionally important in brain networks.

In this Review, we lay out the logic behind null models in network neuroscience. We begin by describing the process of implementing null hypotheses about network features. We then develop a taxonomy of network methods for statistical inference and frame the discussion from a user's perspective. We emphasize null modeling as a process of sampling a wider space of possible networks, and ultimately, a tool for benchmarking the statistical unexpectedness of specific features of interest. Finally, we consider how this flexible framework can be applied to non-standard data types and to emerging questions in the field, such as correlation-based networks and annotated networks.

<sup>1</sup>Institute of Psychiatry, Psychology and Neuroscience, King's College London, London, UK.

<sup>2</sup>Montréal Neurological Institute, McGill University, Montréal, Québec, Canada.

✉e-mail: bratislav.misic@mcgill.ca

<https://doi.org/10.1038/s41583-022-00601-9>

## Modules

Groups of nodes densely connected with each other, but sparsely connected with the rest of the network.

## Null models

Synthetic realizations of brain networks, used to benchmark whether observed network features are statistically unexpected.

## Null hypotheses

The premises that observed relationships between network features are due to chance alone.

## Density

The proportion of possible edges that exist in a network.

## Degree sequence

List of degrees of all nodes in a graph.

## Topology

Logical arrangement of nodes and edges in a network (used in this Review specifically to refer to network topology).

## Network inference

Testing of hypotheses about properties or mechanisms that give rise to observed network features.

## Null models for networks

Suppose that you have access to a new network, representing the brain of a previously unstudied species or the brain of a well-studied species, now reconstructed with unprecedented detail. Using methods from network science, you compute statistics about the network, such as its characteristic path length (the mean of shortest paths among all pairs of nodes) or its clustering coefficient (the proportion of a node's neighbours that are also connected with each other). You find that the network has a path length of 2.5 and a clustering coefficient of 0.3. Are these network features special and specific to your network? Are they unexpectedly large or small in magnitude? Could they have occurred just by chance in a randomly configured network of a similar size?

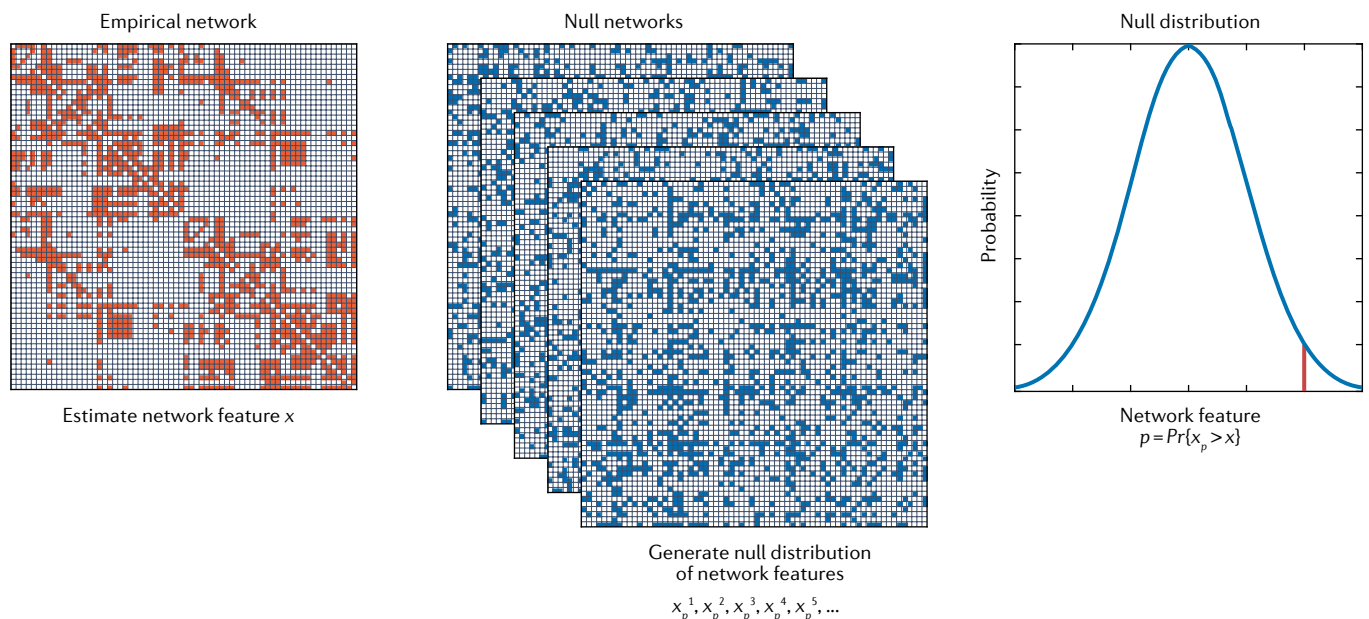
The challenge for network neuroscientists is to benchmark how statistically unexpected a network feature is. Many network features will depend on simpler features, such as the number of nodes (network size), the proportion of possible edges that exist (network density) and the number of edges incident on each node (degree sequence). Topological differences between organisms, populations or experimental conditions may be masked or overemphasized by trivial differences in these basic features. The main inferential process by which we determine that a feature of interest (such as path length or clustering) is due to the topology of our network rather than other features (such as density) is by comparison with null models<sup>20,21</sup>.

FIGURE 1 outlines the process of graph null-hypothesis testing. A network feature ( $x$ ; for example, path length or

clustering coefficient) is first computed on the observed network (red). To assess the statistical significance of this feature, we generate a population of null networks (blue) that preserve some properties of the observed network (in this example, density) but systematically disrupt others (in this example, topology). We then compute the same network feature for each null network, generating a distribution of feature  $x$  ( $x_p$ ) under the null hypothesis that the feature is due to density, as opposed to topology. If the feature of interest  $x$  has significantly greater or smaller magnitude in the observed network than in the null networks, this constitutes evidence that feature  $x$  can be explained by the properties that were not preserved in the null networks. For example, if we find that the observed network consistently displays greater clustering than the null networks with randomized topology but preserved density, we would conclude that the clustering in the observed network is due to topology, rather than density. A  $p$  value is naturally estimated as the proportion of distribution  $x_p$  that is greater than or equal to  $x$ .

## Ubiquity of null models

Null models are so fundamental to network inference that they are effectively subsumed into the very definitions of multiple network measures. For example, the small-world coefficient ( $\sigma$ ), which measures the ratio of clustering ( $C$ ) to path length ( $L$ )<sup>22</sup>, is computed by first normalizing each of these measures according to their average magnitude in a set of randomized networks ( $C_r, L_r$ )<sup>23</sup>:



**Fig. 1 | Generating null distributions for network features.** Graph-theoretic analysis of an observed network (red) can be used to derive a desired feature  $x$ , such as path length, clustering or modularity. Red elements in the matrix represent the presence of a connection and white elements represent the absence of a connection. To determine whether the feature is statistically unexpected, we generate a population of null networks (blue) that preserve some desired properties of the observed network representing null hypothesis  $H_0$  (such as density), but randomize

others that represent hypothesis  $H_1$  (such as topology). Recalculating the same feature  $x$  for each null network allows us to construct a distribution of features  $x_p$  under the null hypothesis that the magnitude of feature  $x$  is due to properties that were preserved, and not due to properties that were randomized. A  $p$  value is then estimated by computing the probability  $\Pr$  that  $x_p$  is more extreme than  $x$ . The figure was generated using an open diffusion MRI and functional MRI data set featuring 70 healthy participants<sup>122</sup>.

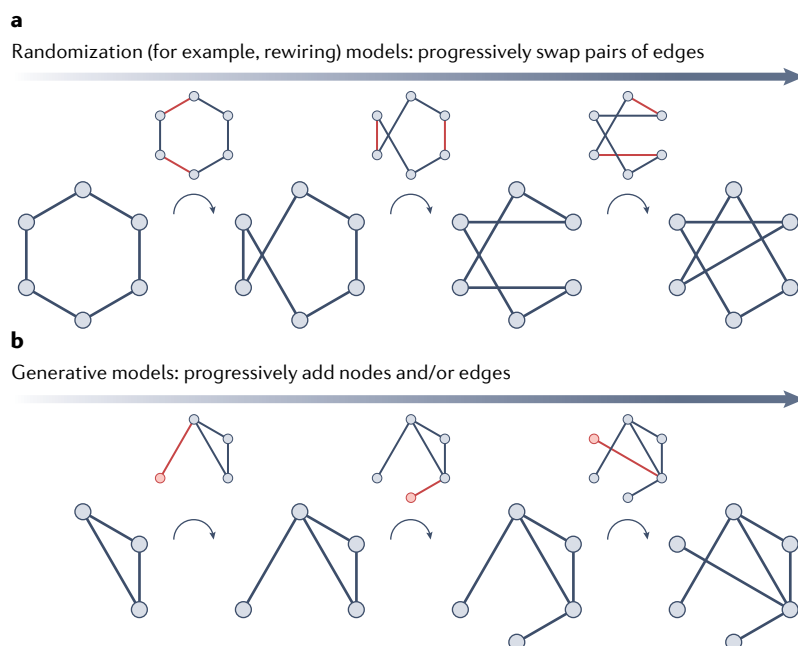


**Fig. 2 | Randomization versus generative models.** All null models systematically disrupt topology of the observed network while retaining other properties, such as density and degree. This procedure is then used to construct a null distribution for features of interest. **a** | A prominent class of network randomization methods is rewiring models that randomly rewired the observed network. Pairs of edges selected at random (red) are swapped, such that edges A–B and C–D now connect A–C and B–D<sup>31</sup>. The goal is to generate rewired networks that have the same numbers of nodes and edges as the observed network, thereby preserving density. Because edges are always swapped (rather than being removed or added), nodes never gain or lose an edge, but have the same number of edges as before the swap. As a result, the rewired network has the same degree sequence as the observed network. Rewired null models can preserve additional properties of the observed network by making edge swaps conditional on other constraints, such as directionality, cost, ratio of intermodular to intramodular edges and so on. **b** | Generative models build a new network from the ground up using a small set of wiring rules. A network is initialized using a subset of nodes and/or edges. New nodes and/or edges are then added pseudorandomly according to a predefined wiring rule that embodies the null hypothesis. The procedure ends when the new network has the same size and density as the observed network. This illustration is shown for synthetic data.

$$\sigma = \frac{C/C_r}{L/L_r} \quad (1)$$

#### Rich club

A group of high-degree nodes disproportionately densely connected with each other.

#### Rewiring

Swapping pairs of edges either randomly or with constraints.

#### Monte Carlo sampling methods

Algorithms that use random sampling to generate numerical estimates of population statistics.

#### Generative models

Procedures for constructing networks by adding edges and/or nodes according to a set of wiring rules.

In another example, the modularity statistic ( $Q$ ) captures how prominent or unexpected within-community links ( $A_{ij}$ ) are in some partition ( $c$ )<sup>24</sup>. The statistic must therefore be defined with respect to a null model that quantifies the expected density of within-community links ( $P_{ij}$ ):

$$Q = \sum_{ij} [A_{ij} - P_{ij}] \delta(c_i, c_j) \quad (2)$$

The degree-preserving configuration model is often used as the null model<sup>24</sup>, although alternative formulations exist<sup>25</sup>, including for signed networks<sup>26</sup> and correlation-derived networks<sup>27</sup>.

As a last example here, the rich club coefficient quantifies the tendency for high-degree nodes in the network to be more densely connected with each other than

would be expected by chance<sup>28,29</sup>. The normalized coefficient ( $\phi_{\text{norm}}$ ) is computed as the ratio of the density of connections among high-degree nodes in a network ( $\phi$ ) and in a population of randomized networks with preserved degree sequences ( $\phi_{\text{rand}}$ ):

$$\phi_{\text{norm}} = \phi / \phi_{\text{rand}} \quad (3)$$

Collectively, these examples — small-worldness, modularity and rich clubs — demonstrate just how ingrained null models are to discovery in network neuroscience. They also demonstrate that null models do not always have to be used purely for testing and rejecting a null hypothesis. Rather, they can be used more broadly, to normalize or benchmark graph statistics relative to a population of networks in which some attributes are controlled or preserved. In other words, null models need not be used exclusively to generate  $p$  values but also to compute  $z$  statistics or to normalize measures. This is particularly desirable in situations in which one wants to compare graphs of different sizes or densities, such as comparative analyses between model organisms that are reconstructed using different methods and at different spatial scales<sup>11</sup> or connectomes reconstructed with personalized parcellations<sup>30</sup>.

### Randomization and generative models

In network neuroscience, and in network science more generally, there exist two distinct ways to construct null networks. All null models embody a null hypothesis by randomizing a property of the observed network, such as topology, while retaining other properties, such as density and degree. Where models differ is how they implement these hypotheses (FIG. 2).

Perhaps the most common network randomization method is rewiring. Rewiring models are a family of Monte Carlo sampling methods that work by randomly rewiring the observed network. Pairs of edges are selected at random (FIG. 2a) and then swapped, such that each edge now connects one ‘old’ node and one ‘new’ node. For example, if we select two edges A–B and C–D, a swap could result in new edges A–C and B–D. The goal is to generate a randomized network that has the same number of nodes and edges as the observed network, thereby preserving density<sup>31</sup>. Importantly, because edges are swapped rather than completely moved, a node can never gain or lose the total number of edges. As a result, the degree of each node is preserved, and the rewired network is said to have the same degree sequence as the original network. This type of null is sometimes referred to as the ‘configuration model’ or Maslov–Sneppen rewiring. As we discuss in the next section, rewired null models can preserve additional properties of the observed network by making edge swaps conditional on other constraints, such as cost<sup>32</sup>, directionality<sup>33,34</sup>, ratio of intermodular to intramodular edges<sup>35</sup> and edge weights<sup>26</sup>.

Whereas rewiring models modify the observed network to generate null networks, generative models build null networks from the ground up (FIG. 2b). A null network is typically initialized using a subset of nodes and/or edges. New nodes and/or edges are then added

pseudorandomly according to a small set of wiring rules that embody the null hypothesis. This construction procedure ends when the null network has the same size and density as the observed network. The specific wiring rules can take many forms. Edges can be placed entirely at random (Erdős–Rényi random graphs<sup>36,37</sup>), to minimize the total edge length (wiring cost) of the network<sup>38,39</sup>, or to maximize homophilic attachment among nodes with similar connectivity profiles<sup>40,41</sup> or similar microscale attributes<sup>42</sup>. More extensive generative growth models may also embody some mechanism by which nodes are added to the network, such as preferential attachment, wherein new nodes are more likely to connect to existing nodes with greater degree<sup>43</sup>. Although generative models primarily aim at uncovering latent principles of organization and growth of empirical networks, they can also be used for hypothesis testing in ways similar to randomization-based null models. In other fields, such as time-series analysis, this distinction is sometimes discussed from the perspective of typical realizations that fit a model to the data (analogous to generative models), versus constrained realizations that are produced by matching one or more properties of the data (analogous to randomization models)<sup>44</sup>.

Generative models can also go beyond significance testing and be used for model identification more generally, by evaluating multiple competing hypotheses about the mechanisms that drive an observed network feature. For example, generative models have been used to test competing accounts of brain network formation: model A (edges are placed to minimize wiring cost only<sup>39</sup>), versus model B (edges are placed among brain regions with overlapping connection profiles<sup>40</sup>) versus model C (edges are placed among regions with similar gene-expression patterns<sup>42</sup>). Models are then compared by assessing how well each of the alternative models (embodying distinct generative mechanisms) recapitulates features of the observed network. This is conceptually similar to model identification in formulations of brain networks as dynamic systems, such as dynamic causal modelling, in which competing accounts of dynamic neural circuit interactions are tested to identify the best-fitting or most parsimonious model<sup>45,46</sup>, or when competing hypotheses are grouped into distinct families of mechanisms or families of models<sup>47</sup>.

Despite differences in implementation, randomization and generative models form a coherent set of analytical tools to formulate and refine hypotheses about network structure. With randomization models, we systematically randomize factors that we hypothesize are important for the network feature we are studying, and retain factors that are hypothesized to not be important. With generative models, we systematically add the minimum set of factors that we hypothesize are important. In this sense, the difference between randomization and generative models is analogous to the difference between non-parametric and parametric tests in statistics. With generative models, as in parametric tests, we explicitly define the data-generating process and assume that the null distribution can be captured by a small set of parameters. With randomization models, as in non-parametric tests, we do not make assumptions about the

null distribution, and instead assemble a null distribution from the observed data using some randomization procedure. Over time, as randomization models gradually become more conservative, they can help to narrow down hypotheses and help to inform generative models.

So far in this Review, we have focused on the randomization of network topology through rewiring or generative modelling. However, null models can also be used to disentangle the interdependence of network properties at other steps in the network construction and analysis pipeline, a topic that we consider in greater detail in the sections on null models for annotated and correlation networks below. For example, use of the correlation coefficient to quantify relationships between pairs of neurophysiological time series during functional-network construction leads to an abundance of fully connected triplets of nodes (owing to the transitive property); in this scenario, a null model involving randomization of time series may be more realistic than randomizing network topology<sup>48</sup>. Similarly, when evaluating relationships between pairs of nodal brain maps, one of the maps can be directly randomized at the level of nodal features while preserving certain properties (such as spatial autocorrelation), without the need to rewire the underlying networks at the level of edges<sup>49</sup>.

### A sampling space of networks

Given the numerous choices of null models available, how do we select the appropriate model as a frame of reference for our observed network? FIGURE 3 shows an observed network, and three different null models that preserve increasingly more of its features. The first null is a random graph, in which only density is preserved. The second null is a Maslov–Sneppen rewired null with preserved density and degree sequence. Notice that, compared with the random null, the rewired null has prominent horizontal and vertical streaks that correspond to similar streaks in the observed network, because nodes that were hubs in the observed network remain hubs in the rewired network. The third null, which preserves density, degree and the total wiring cost of the network, displays a similar organization to the observed network. In other words, as we increase the constraints imposed on the null model, we begin to generate more veridical representations of the original graph, yielding a more conservative null model. This leads to stricter tests associated with the identification of more fine-grained effects, which explain progressively smaller amounts of variance in the original data. This example illustrates two important properties of null models. First, null models exist on a spectrum, ranging from liberal to more conservative nulls, depending on the constraints imposed. Second, null models are a method of systematically sampling a larger space of potential networks, and situating the observed network in this space. We expand on these themes below.

Up to this point in this Review, we have implicitly discussed hard constraints; that is, features that are preserved exactly, such as the degree sequence of a network. Yet there exist myriad null models that operate under ‘soft’ constraints that are met only approximately. A straightforward example is how Maslov–Sneppen-like

#### Wiring cost

The total physical length of all edges in the network.

#### Homophilic attachment

The tendency for pairs of nodes to be connected if they have similar characteristics, such as degree, connection profile or microscale attributes.

#### Transitive property

The dependence among the three edges in triangles of nodes when the edges are estimated by statistical association, such as correlations among time series.

#### Spatial autocorrelation

The tendency for spatially proximal brain regions to possess similar attributes.



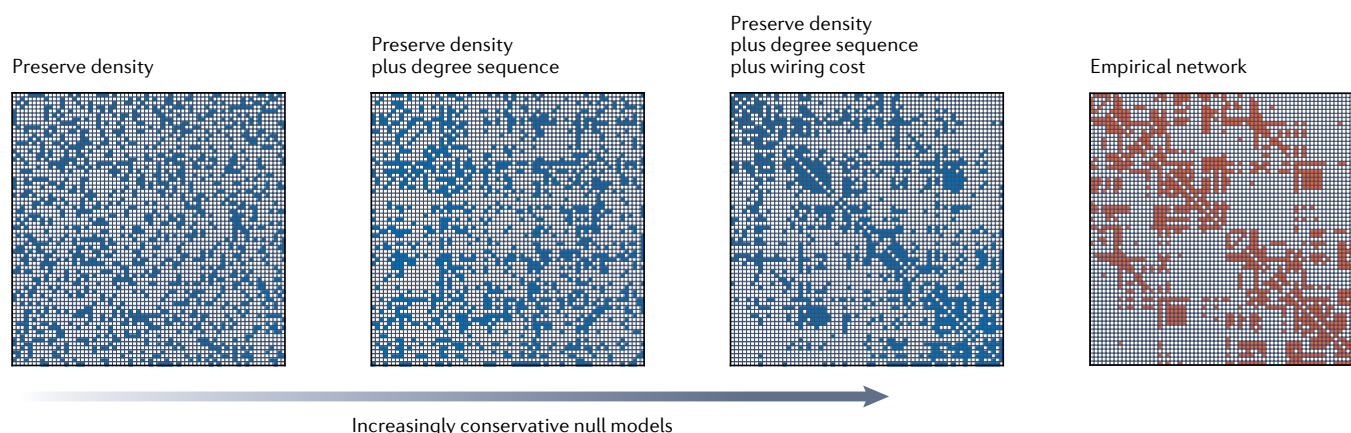


**Fig. 3 | A spectrum of null models.** Null models can be adapted to test a range of hypotheses. The network on the right is an observed empirical network derived from diffusion MRI. Increasing constraints imposed on the model from left to right yield graphs that retain more features from the empirical network, resulting in increasingly conservative null models. In the first null model, an Erdős–Rényi random graph, edges are placed at random such that the network has the same density as the empirical network<sup>36</sup>. In the second null model, using Maslov–Sneppen rewiring,

random edge swapping results in a network with the same density and degree sequence as the empirical network<sup>31</sup>. In the third null model, edges are randomly swapped only if total wiring cost is preserved, resulting in a network with the same density, degree and cost as the empirical network<sup>32</sup>. Visually, the more conservative null models increasingly resemble the observed network because they embody more of its underlying properties. Figure generated using an open diffusion MRI and functional MRI data set featuring 70 healthy participants<sup>122</sup>.

rewiring is applied to weighted networks to approximately preserve the sum of the weights of edges incident on each node (strength sequence)<sup>26</sup>. This procedure involves a first rewiring step that preserves the degree sequence, followed by a second weight-swapping step, in which exact convergence is complicated by the fact that edge weights consist of continuous values that are not perfectly interchangeable. Although the desired constraints are not exactly met in each individual network, they are satisfied, on average, across the ensemble of null networks<sup>50</sup>.

More generally, the process of constructing null models can be thought of as sampling from a broader space of possible networks with related characteristics (FIG. 4). This multidimensional network morphospace is spanned by axes that represent specific network traits or features<sup>31</sup>. Each point or location in this space represents distinct network morphologies, some of which can be realized under desired constraints whereas others cannot. Proximity in this space reflects similarity between network morphologies. The number and stringency of null-model constraints determine the portion of this space that will be populated by null-model instantiations; for example, stringent models will be situated close to the empirical network, whereas increasingly lenient models will tend to be situated further away. Null models — whether realized by rewiring or generative mechanisms — are therefore methods to systematically sample from different parts of this network morphospace and generate null distributions for desired network features. Exploring this space enables us to quantify the contribution of different constraints and generative mechanisms to specific features of our observed network.

A corollary is that the size of the sampling space will influence the variability of null-model realizations. In general, models with additional constraints should theoretically yield realizations that are more similar to each other and hence cover a small portion of the

null-model sampling space. FIGURE 4 demonstrates this concept: null models a, b and c sample increasingly larger spaces of networks, resulting in increasingly variable null distributions. An important methodological question is whether null models uniformly sample the target space. The mere fact that a model retains one feature and randomizes another does not mean that it samples the space of all possible realizations exhaustively. This is directly tied to how null models are implemented in practice, which we consider in the section below about the limits of null models.

Ultimately, there is no right or wrong null model. The null model should be an implementation of an explicit and falsifiable null hypothesis that is specific to one's research question. A variable can be the main independent variable in one study, or a covariate that needs to be controlled for in another. A salient example, which we discuss in detail in the next section, is the contribution of geometric embedding and wiring cost to brain network architecture. The wider space of nulls is a powerful tool to probe the observed network from multiple angles and to parse the contributions of different network properties to the feature of interest (FIG. 4). In this sense, using multiple nulls simultaneously to triangulate towards an answer may be the most comprehensive and informative way to analyse networks<sup>21</sup>.

### Null models for spatial networks

Perhaps the most important feature to consider when analysing brain network topology is geometry<sup>52</sup>. The brain is a spatially embedded system with finite metabolic and material resources, resulting in a prevalence of short-range connections that presumably confer lower cost than do long-range connections<sup>53</sup>. Indeed, multiple imaging modalities and tracing techniques show that neural elements are more likely to be connected and to display stronger connectivity weights if they are physically closer together than if they are further apart<sup>41,54–58</sup>.

#### Network morphospace

A space of network configurations that can be realized under a set of constraints.

#### Geometry

The embedding of nodes and edges in physical space.

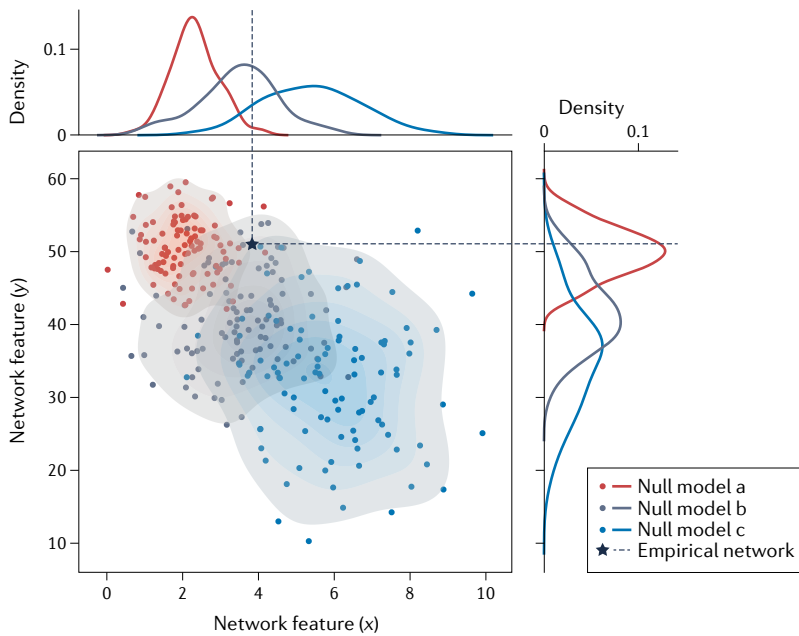


**Fig. 4 | A sampling space of null models.** For any empirical network, we can use multiple null models to systematically sample alternative network configurations. This example shows two network features ( $x$  and  $y$ ) estimated for an empirical network (black star). Three distinct null models (a, b and c) are then used to construct null distributions for each feature (red, purple and blue probability densities, respectively). Situating the empirical network in this space enables systematic and detailed phenotyping of its features. This illustration is shown for synthetic data.

Therefore, connectivity and geometry are fundamentally intertwined, necessitating null models that can selectively tease apart their contributions.

The principal difficulty with using standard rewiring models is that naive swapping will, on average, place edges between nodes that are further apart, yielding null networks with unrealistically higher wiring costs than the observed network. One approach is to use iterative rewiring with additional constraints. Early studies proposed to ‘latticeize’ the observed network; here, the spatial positions of network nodes are taken into account while swapping edges. Candidate edge swaps are implemented only if they place edges between spatially proximal neighbours, creating lattice-like networks<sup>22,33</sup>. Although latticeization reduces the wiring length of the rewired network, more sophisticated versions of this algorithm create rewired networks that precisely match the edge length distribution<sup>59</sup> and the weight–length relationship<sup>32,54</sup> of the observed network, in addition to density and the degree sequence. Further alternative models have used so-called spatially repositioned nulls, in which the spatial locations of the nodes are permuted but the topology is preserved, enabling researchers to assess whether the observed network feature is driven by spatial relationships among nodes, rather than topology<sup>60,61</sup>.

Collectively, geometric nulls enable us to quantify the proportion of topology that comes passively from spatial embedding. For example, purely geometric models that minimize wiring cost can reproduce multiple hallmarks of brain networks, including the presence of hubs<sup>62</sup>, network cores<sup>39</sup> and modules<sup>54,62</sup>. As a result, these nulls

provide a platform to ask whether additional structure in the network can be explained by specific wiring rules. In particular, generative models may include both geometric and topological rules, in which edges are probabilistically placed if they minimize wiring cost and if they additionally optimize some other topological property<sup>63</sup>, such as homophilic attachment<sup>40</sup>. In these models, the influences of geometric and topological constraints are parametrically tuned, enabling researchers to titrate and assess the contribution of each to the overall network architecture. More recently, generative models have begun to consider the joint influence of geometry, topology and local biological annotations of network nodes, such as gene expression or laminar differentiation<sup>42,64</sup>, a topic that we consider further in the next section.

### Null models for annotated networks

The graph representation of the brain deliberately abstracts away microscale differences between regions, resulting in homogeneous nodes. However, network neuroscience is increasingly focused on the relationship between network architecture and regional annotations<sup>65</sup>, such as neuron morphology<sup>66</sup>, gene expression<sup>67,68</sup>, receptor profiles<sup>69</sup>, laminar differentiation<sup>70,71</sup>, myelination<sup>72</sup> and intrinsic dynamics<sup>73</sup>. A typical comparison may involve correlating, across brain regions, a region’s network attribute (such as degree) and its microscale annotation (such as the average number of dendritic spines). However, an important problem arises when estimating a  $p$  value for the correlation coefficient. Namely, the standard parametric method assumes that the two vectors come from an uncorrelated bivariate normal distribution, whereas the non-parametric (naïve permutation-based) method assumes that the elements of the vectors are exchangeable. This independence assumption is violated by multiple forms of dependence between data points<sup>74–76</sup>. First, spatial autocorrelation of imaging data gives rise to similar values of anatomical and physiological measurements between neighbouring locations. Second, homotopic symmetry leads to similar measurements between corresponding locations within the left and right hemispheres of the brain. Last, the spatial resolution of analyses is arbitrary, leading to dependence of both the  $p$  value and the effect size on the number of regions, vertices or voxels considered. These limitations can be addressed using null models that control for spatial autocorrelation, including both spatial permutation tests and parameterized data models<sup>49,77</sup>.

Spatial permutation tests, also known as ‘spin tests’, randomize the relationship between network structure and annotations by randomly rotating spherical projections of brain annotation maps (FIG. 5). These models project brain regions or vertices to a sphere using spherical coordinates generated during cortical-surface extraction. Following random rotation of the sphere, a permutation is obtained by assigning each coordinate to its nearest rotated counterpart. By applying the same (mirrored) random rotation to both brain hemispheres, spatial permutation models also (approximately) preserve hemispheric symmetry. The end result is an annotated graph in which the network structure is preserved

**Surrogate**

Realization of a null model. Mainly used to refer to null time series, but frequently to networks as well.

**Matrix**

A table in which rows and columns correspond to network nodes, and every element encodes a relationship between two nodes, such as connectivity or physical distance.

and the spatial autocorrelation of the annotations is preserved, but the correspondence between network nodes and annotations is randomized (FIG. 5). This test was initially developed at the level of surface vertices<sup>74,75</sup> and subsequently extended to the region level — that is, for parcellated data<sup>78–81</sup>. Notably, different implementations of spatial permutation models at the regional level diverge in specific methodological decisions, such as how to deal with the medial wall or whether they enable annotation values to be assigned more than once<sup>49</sup>.

By contrast, parameterized data models generate surrogate brain maps with predefined spatial properties, such as the same spatial autocorrelation as the empirical data set. Parameterized models do not rely on spherical permutation of data; instead, these models use a matrix of distances between brain-map locations to impose spatial autocorrelation — as described using a parsimonious set of parameters — on randomly permuted data. Several parameterized methods have been proposed, including spatial autoregressive models<sup>82</sup>, smoothing of randomized values to match the empirical variogram<sup>76</sup> and spatial eigendecomposition using Moran spectral randomization<sup>83</sup>. For a systematic comparison of spatial permutation and parameterized data models, see REF.<sup>49</sup>.

Similar to geometric models, spatial autocorrelation-preserving null models enable us to ask to what extent network features occur above and beyond the background influence of spatial embedding. As a result, these models are quickly becoming ubiquitous and can be applied to a wide range of analytical questions. One such application is to assess whether a particular node attribute  $x$  (for example, degree) is enriched in a particular class of nodes (such as in an intrinsic network or cytoarchitectonic class)<sup>68,84,85</sup>. Here the annotations (classes) are categorical variables, and the null model can be used to quantify how unexpectedly large the attribute  $x$  is while controlling for the size and spatial extent of the class. An alternative application is to assess whether nodes with similar annotations display greater than expected connectivity<sup>69,73,86</sup>. In this type of analysis, the mean connectivity among nodes with a particular annotation is compared against a null distribution of

connectivity constructed by rotating annotations. More broadly, these methods have been extended to address the effect of spatial autocorrelation in diverse biological questions, such as within-participant correspondence of neuroimaging modalities<sup>87</sup> or gene-set enrichment<sup>76,88,89</sup>.

**Null models for correlation networks**

Connectivity is often estimated using measures of statistical covariation between regional attributes, such as correlations among measurements of neural activity, gene expression or cortical thickness. Examples of correlation-derived networks include functional networks<sup>90</sup>, structural covariance networks<sup>91,92</sup>, morphometric similarity networks<sup>93</sup>, gene co-expression networks<sup>94</sup>, neuroreceptor similarity networks<sup>69</sup> and temporal profile similarity networks<sup>73</sup>. These networks are weighted (and generally signed) by construction<sup>26</sup>, suggesting that null models that operate at the level of binary topology, such as rewiring models, might be inappropriate. In particular, networks constructed by correlation obey the transitive property: if we know the value of edges A–B and A–C, we can place limits on the value of edge B–C. Rewiring may swap edges in such a way that does not preserve this transitive property — for example, with strong positive correlations between A and B and between A and C, but weak or negative correlation between B and C. Thus, topological rewiring of edges in such networks may result in null networks that could not have arisen naturally as a correlation network<sup>48</sup>. In other words, correlation-derived networks necessitate alternative null models that take into account the transitive property and the sign of edge weights.

Various methods can be used to create more realistic null models for correlation-derived brain networks. One option is to create null correlation matrices, using methods such as the Hirschberger–Qi–Steuer algorithm that matches the mean and variance of the empirical matrix<sup>48,95,96</sup>, or a configuration model that preserves empirical node strength<sup>97</sup>. A more stringent approach is to randomize the signal itself. For example, in the case of functional connectivity, surrogate time series can be generated by transforming empirical time series to the

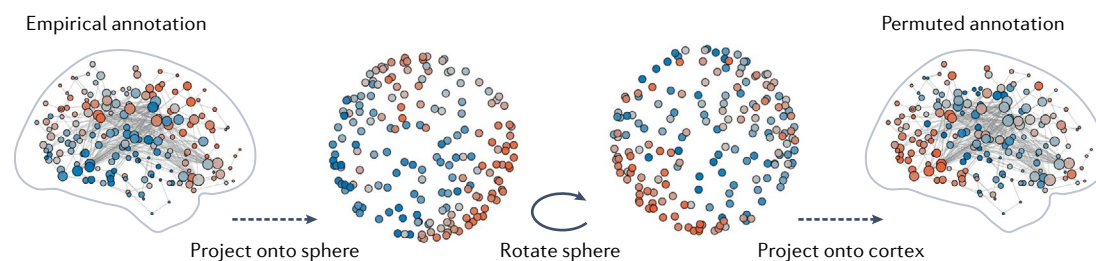


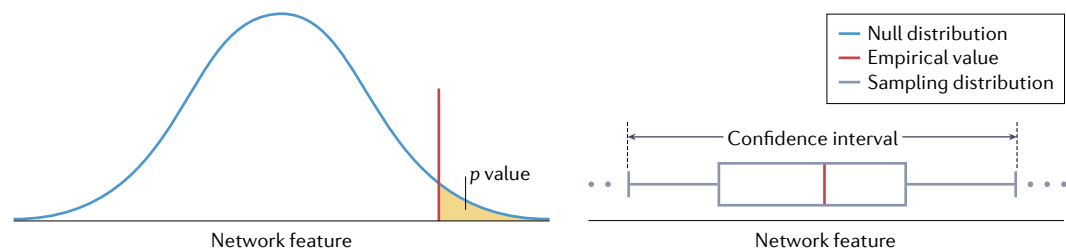
**Fig. 5 | Spatial permutation of network annotations.** When evaluating correspondence between network architecture and local node annotations (such as molecular or cellular attributes), a spatial null model can be used to permute node annotations while preserving their autocorrelation structure<sup>49</sup>. Spatial permutation can be implemented using a ‘spin test’, whereby the annotation map for each hemisphere is projected onto a sphere, randomly rotated and projected back onto cortex. Such permutations approximately preserve spatial autocorrelation and hemispheric symmetry of empirical values or annotations, but systematically randomize correspondence between network structure and annotations. This illustration is generated using glycolytic indices<sup>123</sup> mapped to network nodes defined in REF.<sup>124</sup> as annotation data (shades of red and blue). Edges correspond to an anatomical connectome from REF.<sup>125</sup> (connectivity data are available at REF.<sup>126</sup>). Node sizes are proportional to weighted node connectivity strength, calculated from the connectivity data. Data are shown for left hemisphere only.

### Box 1 | Bootstrapped brain networks

If a slightly different sample of participants was used to estimate anatomical covariance, what would the resulting network look like? If the properties of network nodes differed, how would this affect the degree sequence? More generally, what is our confidence in estimates of connectivity or downstream network statistics? Such questions can be answered using resampling methods such as bootstrapping<sup>128</sup>. Whereas the randomization methods we discuss in the main text are used to generate a null distribution for network features, bootstrapping can be used to generate sampling distributions for network features and estimate their confidence intervals (see the figure). With randomization, we seek to construct a distribution of some data feature that embodies the null hypothesis, and use this procedure to estimate a *p* value. With bootstrapping, we seek to construct confidence intervals, to identify stable features that are insensitive as to which data points are in the sample.

Bootstrapping consists of random sampling with replacement of observations to estimate measures of spread of network statistics (for example, resampling participants A, B, C, D could result in a new sample A, C, D, C). Many statistical approaches used in network neuroscience generate a single quantity, without an associated estimate of variance, or confidence interval. For example, correlation of regional anatomical measurements across a group of participants leads to a single structural covariance network<sup>91,92</sup>. The network can be bootstrapped by drawing equally sized samples of participants with replacement, whereby a single sample will tend to contain multiple instances of some participants, whereas other participants will be missing. Repeated sampling helps identify edges or network features that are stable or insensitive to the specific composition of the sample.

Bootstrapping has been used to quantify the stability of network estimates and derived statistics<sup>129</sup> as well as to threshold networks by retaining edges that are consistently of the same sign (that is, positive or negative) across samples, in both structural covariance<sup>78</sup> and functional brain networks<sup>122</sup>. Bootstrapping of cortical parcellations has also been used to estimate the variance in functional-network statistics and accurately identify individuals using functional-connectome fingerprinting<sup>130</sup>. Last, bootstrapping of network nodes has been used to efficiently estimate, and quantify the uncertainty of, node centrality<sup>131</sup>, motif counts<sup>132</sup> and degree sequences<sup>133</sup> in large networks. Some of these applications have so far been limited to social or gene-regulatory networks, but there is substantial potential for their use in network neuroscience.



frequency domain using the Fourier transform, shuffling the phase coefficients and taking the inverse transform to the time domain. The resulting surrogate time series have preserved power spectra but randomized temporal dependencies<sup>48,98</sup>. This can also be accomplished using the wavelet transform, a procedure known as 'wave-strapping'<sup>99</sup>. Finally, emerging methods from graph signal processing can generalize classical signal operations, such as the Fourier and wavelet transforms, to networks<sup>100</sup>. These methods generate surrogate signals that preserve the smoothness of the observed network<sup>101</sup>.

In addition to randomization, surrogate time series can also be created using generative approaches. For instance, autoregressive models can generate surrogate time series that preserve the temporal (auto)correlation, power spectral density, cross-power spectral density and amplitude distribution of empirical data<sup>102–104</sup>. Although these generative models exclusively preserve temporal features, more recent hybrid models also preserve spatial features. These models generate surrogate time series that preserve spatial autocorrelation<sup>105</sup>, or time series that preserve both spatial and temporal autocorrelation<sup>106</sup>. Beyond human imaging data, sophisticated null models for multi-neuron firing-rate recordings can simultaneously preserve the covariance across time, neurons and experimental conditions<sup>107,108</sup>.

In the case of networks of covarying anatomical attributes, the anatomical measures can simply be randomized

across regions (within participants) because — unlike time series — data points from different participants are independent<sup>96</sup>. In this sense, resampling with replacement (bootstrapping) can also be applied to correlation-based networks to assess the reliability of network features rather than to test a null hypothesis per se (BOX 1). Note that networks estimated using alternative measures of covariation, such as partial correlation, may be less susceptible to interdependencies among edge values induced by the transitive property<sup>48,109–112</sup>. However, such networks should also be evaluated using null models that take into account the fact that their edges represent statistical associations between node attributes.

Collectively, these methods showcase an important point: that some types of networks can be randomized at different levels of the construction and analysis pipeline (FIG. 6). Whereas null models for structural networks and annotated networks tend to operate on the edges or nodes of the networks themselves, many null models for correlation networks can additionally operate at earlier steps in network construction, such as the correlation of physiological time series or anatomical feature vectors. Application of a null model at an early stage of network construction can still be used to generate randomized instances of derived statistics, by applying the analysis workflow to the randomized input data. For example, randomized surrogate time series can be used to

#### Phase coefficients

The offsets or temporal dependencies among sinusoidal components of a time series following a Fourier transform to the frequency domain.



construct a correlation matrix, a binary network and a map of regional node degree, each randomized relative to their empirical counterparts (FIG. 6). Alternatively, the empirical correlation matrix (or derived binary topology or node attribute) could be randomized directly (FIG. 6). Crucially, these different null models can be evaluated simultaneously, to benchmark empirical features of interest more comprehensively.

### Limits of null models

Although null models are the backbone of the scientific method in network neuroscience, they are subject to important theoretical and practical caveats. Relationships between network properties can make it difficult to disentangle their unique and shared contributions to overall network architecture. Namely, the presence of some features may induce the presence of other features, making it impossible to selectively randomize one while keeping others fixed. For example, the concurrence of segregated modules and disproportionately highly connected hub nodes may induce structural by-products, such as hierarchies and rich clubs<sup>50</sup>. Therefore, null-model testing cannot always unambiguously recover the causal structure among network features.

More generally, the freedom to construct spectra of null models necessitates careful interpretation of results relative to underlying assumptions. Overly lenient null models that control too few network attributes give rise to trivial ‘straw man’ arguments that are easy to reject but cannot precisely identify the origin of effects of interest. Conversely, overly stringent null models that simultaneously control too many network attributes may, ultimately, constrain the sampling space of network architectures, resulting in too close a match to the empirical network and limiting insight. This does not mean that the lenient or stringent limits of the spectrum of null models are uninteresting or should not be explored. Rather, these limits should be considered alongside other null models whenever possible to comprehensively characterize the contribution of multiple network attributes.

A related consideration is how well null models actually sample the space that they seek to explore. Namely, null models may systematically undersample or oversample certain locations of the target space. A relevant example is the spin test for annotated networks, which only explores a limited region of the space of networks with preserved spatial autocorrelation. By exactly permuting regional annotations, the spin test has fewer

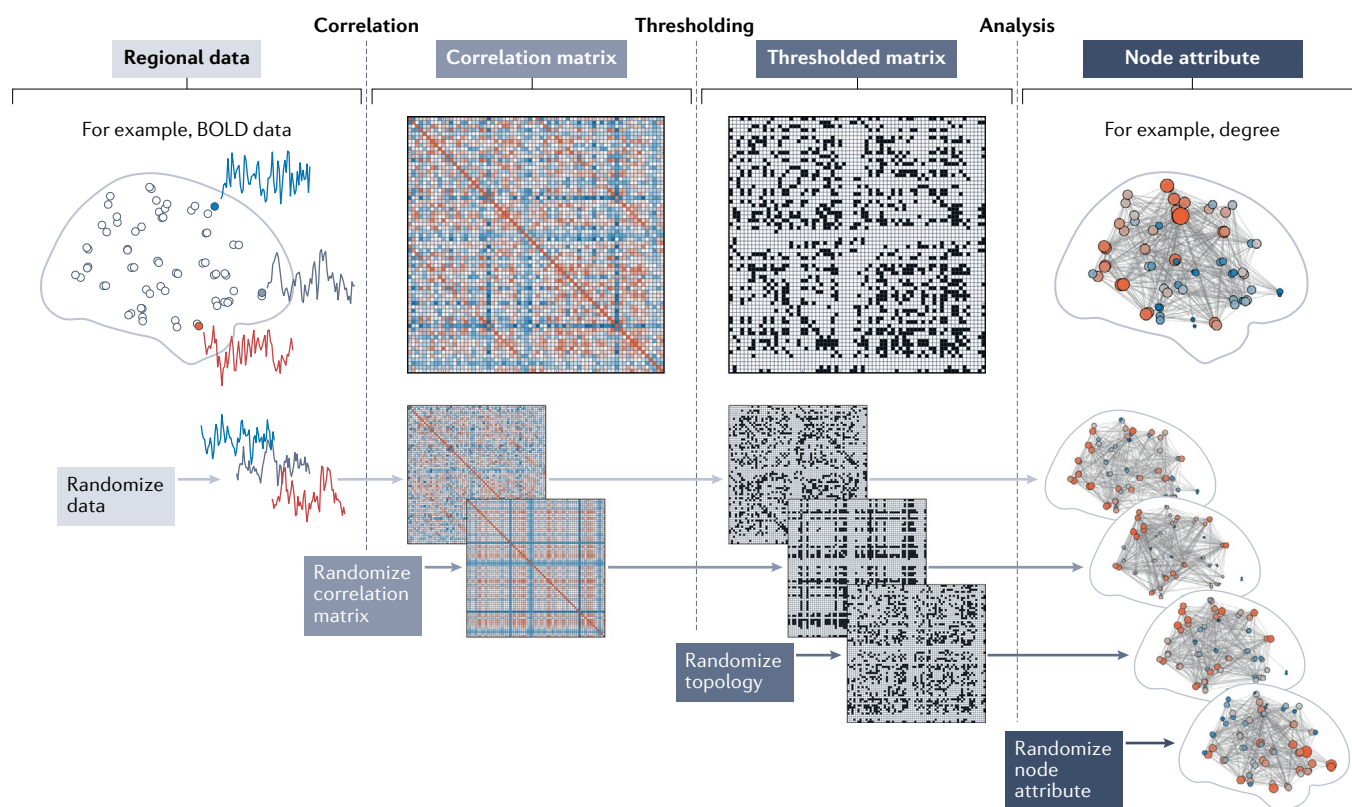


**Fig. 6 | Null models can be implemented at different stages of network construction and analysis.** Brain network construction and analysis involves numerous steps; an example pipeline involves construction of functional connectivity from regional time series, proportional thresholding (25% density) and subsequent topological analysis. A null model could be implemented at every stage of this process, including randomization of time-series data (preserving power spectra), correlation matrix (preserving mean and variance), network topology (preserving node degree) and node attributes

(preserving spatial autocorrelation). Because each null model is applied at a different stage of the workflow, there are multiple ways to generate randomized entities, in which some are randomized directly, and others are considered randomized because an entity at a previous stage of the pipeline was randomized. For example, both time-series randomization and spin nulls may, ultimately, yield randomized node-attribute maps. Illustration generated using functional MRI data (blood oxygen level-dependent (BOLD) responses) from REF.<sup>127</sup>.

possible realizations compared with a parameterized generative model<sup>76</sup>, or compared with a wavelet-based resampling approach in which data are first whitened and then permuted<sup>99</sup>. This example also highlights how randomizations cover a tighter portion of the sampling space of null models, whereas comparable generative model realizations show greater variability, while preserving the quantity of interest in the limit of infinite sampling.

The diversity of null models also brings practical considerations for users. Algorithmic implementations of a null model often imply specific assumptions, which can translate into non-trivial differences in outcomes. For example, different versions of the spin test differ in how they identify the centroid of a region of interest, and whether they permit duplicate assignments during the mapping of spatially randomized region coordinates to the original ones<sup>49</sup>. This variability between different implementations of the same null model can result in differences in inference<sup>49</sup>.

Details of algorithmic implementation can matter even within a specific null model version. It is important to sample null-model instances as uniformly as possible, to ensure that the resulting statistics are not biased. For example, early implementations of the spin test naively used random rotations around the  $(x,y,z)$  axes<sup>75,78</sup>; however, this led to oversampling of certain rotations, unlike the unbiased approach based on QR decomposition of standard normal rotation matrices (factorizing the rotation matrix into an orthogonal matrix  $Q$  and an upper triangular matrix  $R$ )<sup>113,114</sup>. Both aforementioned examples on algorithmic implementation details highlight an important point: deciding what network feature or features to randomize is not sufficient; deciding how this randomization is implemented is important, too. This underlines the importance of sharing code underlying the selected null model implementation and clearly reporting the relevant details<sup>10</sup>.

We finally note that some questions in network neuroscience do not necessarily require benchmarking with null models. If the goal of a study is to generate a feature of brain networks that differentiates groups of individuals (such as patients and controls) or predicts individual differences in some exogenous feature (such as symptom severity), it is more important to show that the feature predicts individual differences in unseen data, rather than to confirm that the feature is statistically unexpected. In other words, comparing a feature in empirical and surrogate data is not informative about its clinical or, more generally, predictive utility<sup>104,115</sup>.

### Outlook and conclusion

We close this Review by considering outstanding questions for next-generation inferential methods in network neuroscience. As the field moves beyond descriptive statistics of brain networks towards understanding generative mechanisms, null models will be key for distilling the smallest set of rules or constraints that can parsimoniously explain the hallmark features of brain networks and their phylogeny and ontogeny. We envisage that the emerging integration of geometric and microarchitectural constraints with existing topological models will

lead to more complete and powerful nulls that can more accurately pinpoint the origin of observed phenomena. These hybrid models will help evaluate the relative importance of canonical brain network features (such as modules, hubs and rich clubs) and, ultimately, illuminate a 'feature hierarchy' that separates unique features of the brain from those that are by-products<sup>50</sup>. Key to this endeavour will be paradigms in which ensembles of null models combinatorially constrain one or more features, to systematically test which features arise as by-products of others.

An important but underexplored direction is to subtly perturb observed networks and explore alternative realizations of brain networks that retain many empirical features. In network neuroscience, null networks are typically created through complete randomization, and, conversely, generative models are typically fully completed. However, both processes can be paused incrementally to explore the immediate vicinity of an empirical network in null-model space, thereby giving insight into the stochastic neighbourhood of brain networks. Such 'connectome mutagenesis' can offer insight into pathological perturbations involved in psychiatric and neurological disorders<sup>116</sup>. Parametrically tuning the extent of randomization in this way can be used to systematically map the space of possible network realizations and to illuminate how trade-offs among biological constraints manifest as network features and architectures<sup>51,117</sup>.

More broadly, null models are the ideal vehicle for forging links and establishing a common language in the neuroscience community and with adjacent fields. Indeed, many of these methods originate from other domains, such as astrophysics<sup>118</sup>, time-series analysis<sup>119</sup>, ecology<sup>120</sup> and bioinformatics<sup>31</sup>. The dominant framework in network neuroscience revolves around the use of null models for null-hypothesis testing. As prediction and cross-validation become dominant frameworks elsewhere in the natural sciences and engineering, a major new frontier is to formulate models that predict the presence and prominence of specific network features in unseen data. In this sense, generative models that are validated out-of-sample present a promising step in the continued evolution of network-neuroscience null models<sup>42</sup>.

From a more pragmatic perspective, standardized reporting of results with respect to multiple null models will promote more comprehensive scientific communication<sup>121</sup>. We encourage readers to explore these methods in their own work; Supplementary Table 1 shows existing cutting-edge implementations of various randomization and generative null models, in Python, MATLAB and R programming languages. Going forward, null models present a unique opportunity to transparently share methods and harmonize analytical frameworks. In turn, this will stimulate widespread adoption of null-model methods and their continued development.

This is an exciting time for network neuroscience. Rapid methodological development enables us to explicitly define falsifiable null hypotheses in the form of null models. Null models, in turn, enable us to ask specific

and increasingly diverse questions about brain network organization. The continued development of null models drives cycles of discovery. At every step or iteration, data are tested against increasingly more sophisticated null models that spark new insights, prompt theoretical and methodological innovation and, ultimately, lead to

more informative network features and null models. As the repertoire of inferential methods grows, so will our understanding of the principles governing brain network organization.

Published online 31 May 2022

1. Sporns, O., Tononi, G. & Kötter, R. The human connectome: a structural description of the human brain. *PLoS Comput. Biol.* **1**, e42 (2005).
2. Bullmore, E. & Sporns, O. Complex brain networks: graph theoretical analysis of structural and functional systems. *Nat. Rev. Neurosci.* **10**, 186–198 (2009).
3. DeWeerd, S. How to map the brain. *Nature* **571**, S6 (2019).
4. Sporns, O. The future of network neuroscience. *Netw. Neurosci.* **1**, 1–2 (2017).
5. Insel, T. R., Landis, S. C. & Collins, F. S. The NIH Brain Initiative. *Science* **340**, 687–688 (2013).
6. Amunts, K. et al. The Human Brain Project: creating a European research infrastructure to decode the human brain. *Neuron* **92**, 574–581 (2016).
7. Bassett, D. S. & Sporns, O. Network neuroscience. *Nat. Neurosci.* **20**, 353–364 (2017).
8. Sejnowski, T. J., Churchland, P. S. & Movshon, J. A. Putting big data to good use in neuroscience. *Nat. Neurosci.* **17**, 1440–1441 (2014).
9. Rubinov, M. & Sporns, O. Complex network measures of brain connectivity: uses and interpretations. *Neuroimage* **52**, 1059–1069 (2010).
10. Poldrack, R. A. et al. Scanning the horizon: towards transparent and reproducible neuroimaging research. *Nat. Rev. Neurosci.* **18**, 115–126 (2017).
11. Van den Heuvel, M. P., Bullmore, E. T. & Sporns, O. Comparative connectomics. *Trends Cogn. Sci.* **20**, 345–361 (2016).
12. Passingham, R. E., Stephan, K. E. & Kötter, R. The anatomical basis of functional localization in the cortex. *Nat. Rev. Neurosci.* **3**, 606–616 (2002).
13. Mars, R. B., Passingham, R. E. & Jbabdi, S. Connectivity fingerprints: from areal descriptions to abstract spaces. *Trends Cogn. Sci.* **22**, 1026–1037 (2018).
14. Sporns, O., Honey, C. J. & Kötter, R. Identification and classification of hubs in brain networks. *PLoS ONE* **2**, e1049 (2007).
15. Van Den Heuvel, M. P., Kahn, R. S., Goñi, J. & Sporns, O. High-cost, high-capacity backbone for global brain communication. *Proc. Natl Acad. Sci. USA* **109**, 11372–11377 (2012).
16. Hilgetag, C.-C., Burns, G. A., O'Neill, M. A., Scannell, J. W. & Young, M. P. Anatomical connectivity defines the organization of clusters of cortical areas in the macaque and the cat. *Philos. Trans. Roy. Soc. Lond. B* **355**, 91–110 (2000).
17. Sporns, O. & Betzel, R. F. Modular brain networks. *Annu. Rev. Psychol.* **67**, 613–640 (2016).
18. Sporns, O. Network attributes for segregation and integration in the human brain. *Curr. Opin. Neurobiol.* **23**, 162–171 (2013).
19. Chung, J. et al. Statistical connectomics. *Annu. Rev. Stat.* **8**, 463–492 (2021).
20. Fornito, A., Zalesky, A. & Bullmore, E. *Fundamentals of Brain Network Analysis* Ch. 10 (Academic, 2016).
21. Klimm, F., Bassett, D. S., Carlson, J. M. & Mucha, P. J. Resolving structural variability in network models and the brain. *PLoS Comput. Biol.* **10**, e1003491 (2014). **This study proposes to comprehensively benchmark observed networks with respect to a spectrum of null models, thereby providing a more complete feature profile.**
22. Watts, D. J. & Strogatz, S. H. Collective dynamics of 'small-world' networks. *Nature* **393**, 440–442 (1998).
23. Humphries, M. D. & Gurney, K. Network 'small-worldness': a quantitative method for determining canonical network equivalence. *PLoS ONE* **3**, e0002051 (2008).
24. Newman, M. E. & Girvan, M. Finding and evaluating community structure in networks. *Phys. Rev. E* **69**, 026113 (2004).
25. Esfahani, F. Z. et al. Modularity maximization as a flexible and generic framework for brain network exploratory analysis. *Neuroimage* **244**, 118607 (2021).
26. Rubinov, M. & Sporns, O. Weight-conserving characterization of complex functional brain networks. *Neuroimage* **56**, 2068–2079 (2011).
27. MacMahon, M. & Garlaschelli, D. Community detection for correlation matrices. *Phys. Rev. X* **5**, 21006 (2015).
28. Colizza, V., Flammini, A., Serrano, M. A. & Vespignani, A. Detecting rich-club ordering in complex networks. *Nat. Phys.* **2**, 110–115 (2006).
29. Alstott, J., Panzarasa, P., Rubinov, M., Bullmore, E. & Vèrtes, P. A unifying framework for measuring weighted rich clubs by integrating randomized controls. *Sci. Rep.* **4**, 7525 (2014).
30. Im, K., Paldino, M. J., Poduri, A., Sporns, O. & Grant, P. E. Altered white matter connectivity and network organization in polymicrogyria revealed by individual gyral topology-based analysis. *Neuroimage* **86**, 182–193 (2014).
31. Maslov, S. & Sneppen, K. Specificity and stability in topology of protein networks. *Science* **296**, 910–913 (2002).
32. Betzel, R. F. & Bassett, D. S. Specificity and robustness of long-distance connections in weighted, interareal connectomes. *Proc. Natl Acad. Sci. USA* **115**, E4880–E4889 (2018). **This study introduces a constrained rewiring model that preserves density and degree sequence, and approximately preserves the connection length distribution and length-weight relationship.**
33. Sporns, O. & Kötter, R. Motifs in brain networks. *PLoS Biol.* **2**, e369 (2004).
34. Kale, P., Zalesky, A. & Gollo, L. L. Estimating the impact of structural directionality: how reliable are undirected connectomes? *Net. Neurosci.* **2**, 259–284 (2018).
35. Suárez, L. E., Richards, B. A., Lajoie, G. & Misić, B. Learning function from structure in neuromorphic networks. *Nat. Mach. Intell.* **3**, 771–786 (2021).
36. Erdős, P. & Rényi, A. On the evolution of random graphs. *Publ. Math. Inst. Hung. Acad. Sci.* **5**, 17–60 (1960).
37. Gilbert, E. N. Random graphs. *Ann. Math. Stat.* **30**, 1141–1144 (1959).
38. Kaiser, M. & Hilgetag, C. C. Nonoptimal component placement, but short processing paths, due to long-distance projections in neural systems. *PLoS Comput. Biol.* **2**, e95 (2006).
39. Ercey-Ravasz, M. et al. A predictive network model of cerebral cortical connectivity based on a distance rule. *Neuron* **80**, 184–197 (2013).
40. Betzel, R. F. et al. Generative models of the human connectome. *Neuroimage* **124**, 1054–1064 (2016).
41. Goulas, A., Betzel, R. F. & Hilgetag, C. C. Spatiotemporal ontogeny of brain wiring. *Sci. Adv.* **5**, eaav6964 (2019).
42. Oldham, S. et al. Modeling spatial, developmental, physiological, and topological constraints on human brain connectivity. Preprint at *bioRxiv* <https://doi.org/10.1101/2021.09.29.462379> (2021).
43. Barabási, A.-L. & Albert, R. Emergence of scaling in random networks. *Science* **286**, 509–512 (1999).
44. Lancaster, G., Iatsenko, D., Pidde, A., Ticcinelli, V. & Stefanovska, A. Surrogate data for hypothesis testing of physical systems. *Phys. Rep.* **748**, 1–60 (2018).
45. Daunizeau, J., David, O. & Stephan, K. Dynamic causal modelling: a critical review of the biophysical and statistical foundations. *Neuroimage* **58**, 312–322 (2011).
46. Roebroeck, A., Formisano, E. & Goebel, R. The identification of interacting networks in the brain using fMRI: model selection, causality and deconvolution. *Neuroimage* **58**, 296–302 (2011).
47. Penny, W. D. et al. Comparing families of dynamic causal models. *PLoS Comput. Biol.* **6**, 1–14 (2010).
48. Zalesky, A., Fornito, A. & Bullmore, E. On the use of correlation as a measure of network connectivity. *Neuroimage* **60**, 2096–2106 (2012). **This statistical study investigates how the transitive property induces topological structure in correlation-based networks.**
49. Markello, R. D. & Misić, B. Comparing spatial null models for brain maps. *Neuroimage* **236**, 118052 (2021). **This benchmarking study compares the performance of ten spatial null models in both simulations and empirical data analysis.**
50. Rubinov, M. Constraints and spandrels of interareal connectomes. *Nat. Commun.* **7**, 13812 (2016). **This modelling study introduces an integrative approach to infer causal relationships among network features.**
51. Avena-Koenigsberger, A., Goñi, J., Solé, R. & Sporns, O. Network morphospace. *J. R. Soc. Interface* **12**, 20140881 (2015). **This article reviews how to chart and explore the space of possible network realizations (network morphospace).**
52. Stiso, J. & Bassett, D. S. Spatial embedding imposes constraints on neuronal network architectures. *Trends Cogn. Sci.* **22**, 1127–1142 (2018).
53. Bullmore, E. & Sporns, O. The economy of brain network organization. *Nat. Rev. Neurosci.* **13**, 336–349 (2012).
54. Roberts, J. A. et al. The contribution of geometry to the human connectome. *Neuroimage* **124**, 379–393 (2016).
55. Markov, N. T. et al. Cortical high-density counterstream architectures. *Science* **342**, 1238406 (2013).
56. Liu, Z.-Q., Zheng, Y.-Q. & Misić, B. Network topology of the marmoset connectome. *Netw. Neurosci.* **4**, 1181–1196 (2020).
57. Liu, Z.-Q., Betzel, R. & Misić, B. Benchmarking functional connectivity by the structure and geometry of the human brain. *Netw. Neurosci.* [https://doi.org/10.1162/netn\\_a.00236](https://doi.org/10.1162/netn_a.00236) (2021).
58. Misić, B. et al. The functional connectivity landscape of the human brain. *PLoS ONE* **9**, e111007 (2014).
59. Samu, D., Seth, A. K. & Nowotny, T. Influence of wiring cost on the large-scale architecture of human cortical connectivity. *PLoS Comput. Biol.* **10**, e1003557 (2014).
60. Seguin, C., Van Den Heuvel, M. P. & Zalesky, A. Navigation of brain networks. *Proc. Natl Acad. Sci. USA* **115**, 6297–6302 (2018).
61. Zheng, Y.-Q. et al. Local vulnerability and global connectivity jointly shape neurodegenerative disease propagation. *PLoS Biol.* **17**, e3000495 (2019).
62. Henderson, J. A. & Robinson, P. A. Relations between the geometry of cortical gyrification and white-matter network architecture. *Brain Conn.* **4**, 112–130 (2014).
63. Vèrtes, P. E. et al. Simple models of human brain functional networks. *Proc. Natl Acad. Sci. USA* **109**, 5868–5873 (2012). **This study uses a generative model to investigate the contribution of geometric and topological wiring constraints to hallmark network features of the brain.**
64. Akarca, D., Vèrtes, P. E., Bullmore, E. T. & Astle, D. E. A generative network model of neurodevelopmental diversity in structural brain organization. *Nat. Commun.* **12**, 1–18 (2021).
65. Vázquez-Rodríguez, B., Liu, Z.-Q., Hagmann, P. & Misić, B. Signal propagation via cortical hierarchies. *Netw. Neurosci.* **4**, 1072–1090 (2020).
66. Scholtens, L. H., Schmidt, R., de Reus, M. A. & van den Heuvel, M. P. Linking macroscale graph analytical organization to microscale neuroarchitectonics in the macaque connectome. *J. Neurosci.* **34**, 12192–12205 (2014).
67. Fulcher, B. D. & Fornito, A. A transcriptional signature of hub connectivity in the mouse connectome. *Proc. Natl Acad. Sci. USA* **113**, 1435–1440 (2016).
68. Hansen, J. Y. et al. Mapping gene transcription and neurocognition across human neocortex. *Nat. Hum. Behav.* **5**, 1240–1250 (2021).
69. Hansen, J. Y. et al. Mapping neurotransmitter systems to the structural and functional organization of the human neocortex. Preprint at *bioRxiv* <https://doi.org/10.1101/2021.10.28.466336> (2021).
70. Goulas, A., Majka, P., Rosa, M. G. & Hilgetag, C. C. A blueprint of mammalian cortical connectomes. *PLoS Biol.* **17**, e2005346 (2019).
71. Shami, I. & Assaf, Y. An MRI-based, data-driven model of cortical laminar connectivity. *Neuroinformatics* **19**, 205–218 (2021).



72. Whitaker, K. J. et al. Adolescence is associated with transcriptionally patterned consolidation of the hubs of the human brain connectome. *Proc. Natl Acad. Sci. USA* **113**, 9105–9110 (2016).
73. Shafiei, G. et al. Topographic gradients of intrinsic dynamics across neocortex. *eLife* **9**, e62116 (2020).
74. Alexander-Bloch, A., Raznahan, A., Bullmore, E. & Giedd, J. The convergence of maturational change and structural covariance in human cortical networks. *J. Neurosci.* **33**, 2889–2899 (2013).
75. Alexander-Bloch, A. F. et al. On testing for spatial correspondence between maps of human brain structure and function. *NeuroImage* **178**, 540–551 (2018).  
**This methodological paper introduces a spatial permutation null model to test for correspondence between brain maps.**
76. Burt, J. B., Helmer, M., Shinn, M., Anticevic, A. & Murray, J. D. Generative modeling of brain maps with spatial autocorrelation. *NeuroImage* **220**, 117038 (2020).  
**This methodological study develops a parameterized model that generates null brain maps with preserved spatial autocorrelation.**
77. Markello, R. D. et al. Neuromaps: structural and functional interpretation of brain maps. Preprint at *bioRxiv* <https://doi.org/10.1101/2022.01.06.475081> (2022).
78. Váša, F. et al. Adolescent tuning of association cortex in human structural brain networks. *Cereb. Cortex* **28**, 281–294 (2018).
79. Vázquez-Rodríguez, B. et al. Gradients of structure–function tethering across neocortex. *Proc. Natl Acad. Sci. USA* **116**, 21219–21227 (2019).
80. Baum, G. L. et al. Development of structure–function coupling in human brain networks during youth. *Proc. Natl Acad. Sci. USA* **117**, 771–778 (2020).
81. Cornblath, E. J. et al. Temporal sequences of brain activity at rest are constrained by white matter structure and modulated by cognitive demands. *Commun. Biol.* **3**, 1–12 (2020).
82. Burt, J. B. et al. Hierarchy of transcriptomic specialization across human cortex captured by structural neuroimaging topography. *Nat. Neurosci.* **21**, 1251–1259 (2018).
83. Wael, R. V. D. et al. BrainSpace: a toolbox for the analysis of macroscale gradients in neuroimaging and connectomics datasets. *Commun. Biol.* **3**, 103 (2020).
84. Bazinet, V., de Wael, R. V., Hagmann, P., Bernhardt, B. C. & Misic, B. Multiscale communication in cortico-cortical networks. *NeuroImage* **243**, 118546 (2021).
85. Shafiei, G. et al. Spatial patterning of tissue volume loss in schizophrenia reflects brain network architecture. *Biol. Psychiatry* **87**, 727–735 (2020).
86. Shafiei, G. et al. Network structure and transcriptomic vulnerability shape atrophy in frontotemporal dementia. *Brain* <https://doi.org/10.1093/brain/awac069> (2022).
87. Weinstein, S. M. et al. A simple permutation-based test of intermodal correspondence. *Hum. Brain Mapp.* **42**, 5175–5187 (2021).
88. Fulcher, B. D., Arnatkeviciute, A. & Fornito, A. Overcoming false-positive gene-category enrichment in the analysis of spatially resolved transcriptomic brain atlas data. *Nat. Commun.* **12**, 2669 (2021).
89. Wei, Y. et al. Statistical testing in transcriptomic-neuroimaging studies: a how-to and evaluation of methods assessing spatial and gene specificity. *Hum. Brain Mapp.* **43**, 885–901 (2021).
90. Hlinka, J., Paluš, M., Vejmelka, M., Mantini, D. & Corbetta, M. Functional connectivity in resting-state fMRI: is linear correlation sufficient? *NeuroImage* **54**, 2218–2225 (2011).
91. Alexander-Bloch, A., Giedd, J. N. & Bullmore, E. Imaging structural co-variance between human brain regions. *Nat. Rev. Neurosci.* **14**, 322–336 (2013).
92. Evans, A. C. Networks of anatomical covariance. *NeuroImage* **80**, 489–504 (2013).
93. Seidlitz, J. et al. Morphometric similarity networks detect microscale cortical organization and predict inter-individual cognitive variation. *Neuron* **97**, 231–247 (2018).
94. Fornito, A., Arnatkeviciūtė, A. & Fulcher, B. D. Bridging the gap between connectome and transcriptome. *Trends Cogn. Sci.* **23**, 34–50 (2019).
95. Hirschberger, M., Qi, Y. & Steuer, R. E. Randomly generating portfolio-selection covariance matrices with specified distributional characteristics. *Eur. J. Oper. Res.* **177**, 1610–1625 (2007).
96. Hosseini, S. M. H. & Kesler, S. R. Influence of choice of null network on small-world parameters of structural correlation networks. *PLoS ONE* <https://doi.org/10.1371/journal.pone.0067354> (2013).
97. Masuda, N., Kojaku, S. & Sano, Y. Configuration model for correlation matrices preserving the node strength. *Phys. Rev. E* **98**, 12312 (2018).
98. Prichard, D. & Theiler, J. Generating surrogate data for time series with several simultaneously measured variables. *Phys. Rev. Lett.* **73**, 951–954 (1994).
99. Breakspear, M., Brammer, M. J., Bullmore, E. T., Das, P. & Williams, L. M. Spatiotemporal wavelet resampling for functional neuroimaging data. *Hum. Brain Mapp.* **23**, 1–25 (2004).
100. Huang, W. et al. A graph signal processing perspective on functional brain imaging. *Proc. IEEE* **106**, 868–885 (2018).
101. Pirondini, E., Vybornova, A., Coscia, M. & Van De Ville, D. A spectral method for generating surrogate graph signals. *IEEE Sig. Proc. Lett.* **23**, 1275–1278 (2016).
102. Chang, C. & Glover, G. H. Time–frequency dynamics of resting-state brain connectivity measured with fMRI. *NeuroImage* **50**, 81–98 (2010).
103. Zalesky, A., Fornito, A., Cocchi, L., Gollo, L. L. & Breakspear, M. Time-resolved resting-state brain networks. *Proc. Natl Acad. Sci. USA* **111**, 10341–10346 (2014).
104. Liégeois, R., Yeo, B. T. T. & Van De Ville, D. Interpreting null models of resting-state functional MRI dynamics: not throwing the model out with the hypothesis. *NeuroImage* **243**, 118518 (2021).  
**This review explores how null models can be applied at different points in the analysis pipeline to identify unexpected features of time-resolved functional brain dynamics.**
105. Esfahlani, F. Z., Bertolero, M. A., Bassett, D. S. & Betzel, R. F. Space-independent community and hub structure of functional brain networks. *NeuroImage* **211**, 116612 (2020).
106. Shinn, M. et al. Spatial and temporal autocorrelation weave human brain networks. Preprint at *bioRxiv* <https://doi.org/10.1101/2021.06.01.446561> (2021).
107. Elsayed, G. F. & Cunningham, J. P. Structure in neural population recordings: an expected byproduct of simpler phenomena? *Nat. Neurosci.* **20**, 1310–1318 (2017).  
**This article introduces a framework to test whether population structure in multi-neuron recordings is a by-product of correlations across time, neurons and experimental conditions.**
108. Pillow, J. W. & Aoi, M. C. Is population activity more than the sum of its parts? *Nat. Neurosci.* **20**, 1196–1198 (2017).
109. Marrelec, G. et al. Partial correlation for functional brain interactivity investigation in functional MRI. *NeuroImage* **32**, 228–237 (2006).
110. Koller, D. & Friedman, N. *Probabilistic Graphical Models: Principles and Techniques* (Academic, 2009).
111. Dadi, K. et al. Benchmarking functional connectome-based predictive models for resting-state fMRI. *NeuroImage* **192**, 115–134 (2019).
112. Liégeois, R., Santos, A., Matta, V., Van De Ville, D. & Sayed, A. H. Revisiting correlation-based functional connectivity and its relationship with structural connectivity. *Netw. Neurosci.* **4**, 1235–1251 (2020).
113. Blaser, R. & Fryzlewicz, P. Random rotation ensembles. *J. Mach. Learn. Res.* **17**, 1–26 (2016).
114. Lefèvre, J. et al. Spanol (spectral analysis of lobes): a spectral clustering framework for individual and group parcellation of cortical surfaces in lobes. *Front. Neurosci.* **12**, 00354 (2018).
115. Zhang, M. The use and limitations of null-model-based hypothesis testing. *Biol. Philos.* **35**, 1–22 (2020).
116. Gollo, L. L. et al. Fragility and volatility of structural hubs in the human connectome. *Nat. Neurosci.* **21**, 1107–1116 (2018).  
**This study implements connectome mutations by parametrically tuning the extent of randomization.**
117. Goñi, J. et al. Exploring the morphospace of communication efficiency in complex networks. *PLoS ONE* **8**, e58070 (2013).
118. Barrow, J. D., Bhavsar, S. G. & Sonoda, D. H. A bootstrap resampling analysis of galaxy clustering. *Monthly Not. Astron. Soc.* **210**, 19P–23P (1984).
119. Theiler, J., Eubank, S., Longtin, A., Galdrikian, B. & Doynne Farmer, J. Testing for nonlinearity in time series: the method of surrogate data. *Phys. D. Nonlinear Phenom.* **58**, 77–94 (1992).
120. Gotelli, N. J. & Graves, G. R. *Null Models in Ecology* (Smithsonian Institution Press, 1996).
121. DuPre, E. et al. Beyond advertising: new infrastructures for publishing integrated research objects. *PLoS Comput. Biol.* **18**, 1–7 (2022).
122. Griffa, A., Alemán-Gómez, Y. & Hagmann, P. Structural and functional connectome from 70 young healthy adults. *Zenodo* <https://doi.org/10.5281/zenodo.2872623> (2019).
123. Vaishnavi, S. N. et al. Regional aerobic glycolysis in the human brain. *Proc. Natl Acad. Sci. USA* **107**, 17757–17762 (2010).
124. Váša, F. et al. Conservative and disruptive modes of adolescent change in human brain functional connectivity. *Proc. Natl Acad. Sci. USA* **117**, 3248–3253 (2020).
125. Rosen, B. O. & Hagmann, E. A whole-cortex probabilistic diffusion tractography connectome. *eNeuro* <https://doi.org/10.1523/ENEURO.0416-20.2020> (2021).
126. Rosen, B. O. & Hagmann, E. A whole-cortex probabilistic diffusion tractography connectome. *Zenodo* <https://doi.org/10.5281/zenodo.4060485> (2020).
127. Senden, M. et al. Task-related effective connectivity reveals that the cortical rich club gates cortex-wide communication. *Hum. Brain Mapp.* **39**, 1246–1262 (2018).
128. Efron, B. & Tibshirani, R. Bootstrap methods for standard errors, confidence intervals, and other measures of statistical accuracy. *Stat. Sci.* **1**, 54–75 (1986).
129. Filosi, M., Visintainer, R., Riccadonna, S., Jurman, G. & Furlanello, C. Stability indicators in network reconstruction. *PLoS ONE* **9**, e89815 (2014).
130. Cheng, H. et al. Pseudo-bootstrap network analysis — an application in functional connectivity fingerprinting. *Front. Hum. Neurosci.* **11**, 351 (2017).
131. Ohara, K., Saito, K., Kimura, M. & Motoda, H. in *Int. Conf. Discovery Sci.* (eds Džeroski, S., Panov, P., Kocov, D. & Todorovski, L.) 228–239 (Springer International, 2014).
132. Bhattacharyya, S. & Bickel, P. J. Subsampling bootstrap of count features of networks. *Ann. Stat.* **43**, 2384–2411 (2015).
133. Gel, Y. R., Lyubchich, V. & Ramirez Ramirez, L. L. Bootstrap quantification of estimation uncertainties in network degree distributions. *Sci. Rep.* **7**, 5807 (2017).

## Acknowledgements

The authors thank A. Goulas for stimulating discussions during the conceptualizing of this work, and E. Suárez, A. Luppi, V. Bazinet, G. Shafiei, J. Hansen, Z.-Q. Liu, O. Sherwood and R. Moran for constructive comments on the manuscript. F.V. acknowledges support from the Data to Early Diagnosis and Precision Medicine Industrial Strategy Challenge Fund, UK Research and Innovation (UKRI) and the Bill & Melinda Gates Foundation. B.M. acknowledges support from the Natural Sciences and Engineering Research Council of Canada (NSERC), the Canadian Institutes of Health Research (CIHR), the Brain Canada Foundation Future Leaders Fund, the Canada Research Chairs Program and the Healthy Brains for Healthy Lives initiative.

## Author contributions

The authors contributed equally to all aspects of the article.

## Competing interests

The authors declare no competing interests.

## Peer review information

*Nature Reviews Neuroscience* thanks M. Breakspear and the other, anonymous referee(s) for their contribution to the peer review of this work.

## Publisher's note

Springer Nature remains neutral with regard to jurisdictional claims in published maps and institutional affiliations.

## Supplementary information

The online version contains supplementary material available at <https://doi.org/10.1038/s41583-022-00601-9>.

© Springer Nature Limited 2022